Electrons and Quantum Tunneling: Barrier properties and their effects on tunneling probability (with applications to transistor design).

Luis Antonio Perez

December 11, 2013

Abstract

Quantum Tunneling is a quantum mechanical occurrence that consists of particles passing through a barrier from Side A to Side B; in technical terms, the wave function of the particle originating on Side A, despite decreasing exponentially while inside the increased potential of the barrier, is non-zero on Side B. This implies a non-zero probability of finding the particle on the "wrong" side of the classically impenetrable barrier.

This effect is observable in practical applications, such as in the construction of miniature transistors. In this paper, we explore this quantum mechanical effect in terms of a single particle encountering a square barrier. This type of model approaches remarkably well that of a transistor in current CPU dies, and we propose a correlation between different insulating materials and the results from our model. In particular, we investigate the effects barrier properties, such as thickness and height, potential landscape differences such as changes in potential from Side A to Side B, and particle properties such as mass and kinetic energy have on the tunneling probability, or as known in the literature, the transmittance ratio. The ratio is found to decrease exponentially with increasing height and width of the potential barrier. It is also found to occur at significant amounts only when the wavelength of the approaching particle is about the same magnitude as the barrier width.

Contents

List of Figures

1 Introduction

It is generally accepted that computers get faster. The trend of increased computational power began with the replacement of the vacuum tube by the transistor, and has continued through improved miniaturization techniques which allow for an increased number of minute metaloxidesemiconductor field-effect transistors (MOSFETs) [10] to be packed into a limited surface area. Modern Intel CPUs, for example, have on the order of a billion transistors per core.

Yet, the idea that computing power will continue to double in potential about once every 18 months, known as Moore's Law [10], is reaching a fundamental quantum mechanical limit. As MOSFET transistors shrink in magnitude, the classical laws of macroscopic objects are joined by the "creepy" effects of microscopic quantum mechanical objects [6]. As the scales of the systems are reduced, these effects become an important factor in determining transistor viability and efficiency.

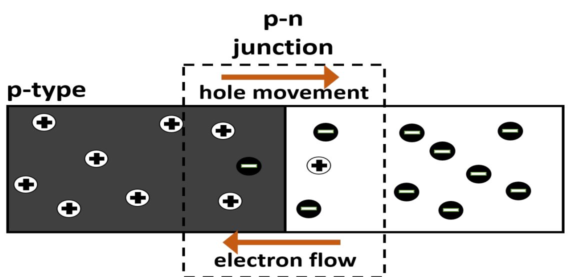

Figure 1: Semiconductors: p-type and n-type junction. Flow of current from left to right only. Such materials allows for controlling current flow in transistors, but quantum tunneling can render the control of current flow achieved by $p - n$ junction useless.

Current MOSFET designs consist of a mixture of n-type and p-type semi-conducting materials which allow for the direct but controlled flow of current. These type of materials, as shown in Figure 1, have unique properties which allow for current flow in only one direction. The flow is directly controlled by an applied voltage to a gate, which is otherwise insulated from the system. This control is what, at a fundamental level, allows computation at the bit level by providing the capacity for logic gate construction. Yet, as the transistors shrink in size, it is necessary for the insulating material between the gate and the conduction band to shrink. The quantum tunneling of electrons through the shrunken insulating barrier leads to inefficient and error-prone transistors. Calculations can no longer be carried out with any level of accuracy, and the computation model breaks down. Therefore, it is of great importance to explore ways in which this type of degradation can be mitigated.

2 Background, Preliminary, and Related Work

The goal of this project is to explore the properties of differing insulating layer thickness as well as different insulating materials. As Figure 2 shows, empirical evidence suggest that as the barrier decreases. Research in this area is plentiful, including the generalization of the system into a mathematically precise model by Simmons and John [2]. This model incorporates not only barrier aspects in the system, but also possible differences in gate/channel material as well as more classical

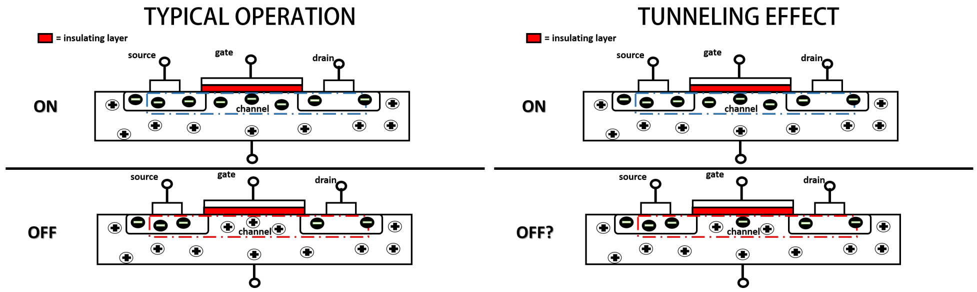

Figure 2: Semiconductors: MOSFET model and electronic tunneling. Image on the left shows operation of transistors at typical size. Note that flow of current through channel is controlled. The image on the right shows faulty operation of transistor after miniaturization (ie, decreased insulating layer thickness). Note that OFF state still allows for current flow.

characteristics such as temperature of operation and permitting of the material. This paper is closely based on their work, and seeks to simplify and provide an intuitive understanding to the effects of quantum tunneling in transistors.

Additionally, research in the area of the utility of electronic tunneling is in the works [3] [4]. It is possible for new transistor types to be fully developed that theoretically improve on our current generation of transistors and allow for a wider range of applications. Yet, research into the area of quantum tunneling in itself remain important, in particular research that allows for intuitive understanding of quantum effects. Therefore, this paper focuses on presenting a simple model of a barrier and on developing the tools necessary to analyze it.

A theoretical model for the particle-barrier system has already been developed [11], but here we chose a slightly modified version consisting of a simple square particle-barrier model. Intuitively, the potential barrier models the insulating layer between the gate and the conductive channel, while each side of the barrier represents the gate and conductive channel respectively. The reason for the square barrier, as opposed to a generalized graduated or inclined potential, is due to the rapid increase in potential that occurs in the actual gate/transistor system as an electron approaches the non-conductive insulating layer. After all, the purpose of the insulator is to block all electrical current from flowing, and can therefore be closely approximated as a square potential barrier.

The main purpose of this paper is to illustrate the results of the investigation into electron tunneling in the described system. By calculating the Schrdinger Wave Function for an electron in our model under different parameters, the probability can be derived and the tunneling effect visualized. By varying the width of our model barrier, changes in the thickness of the insulating material can be mimicked. Furthermore, changes in barrier height are representative of changes in the type of material, and changes in the potential landscape can be used to model dramatic changes in potential energies on either side of the insulating layer in a transistor. Additionally, the model allows for variability in the properties of the particle studied which have direct corresponding physical properties.

3 Intuitive Model of MOSFET System

Tunneling is a purely quantum mechanical phenomena not encountered in classical physics; its existence is due to the wave-particle duality and, more directly, to the Heisenberg uncertainty principal. In classical physics, a particle with energy E_k cannot possibly cross a potential barrier at energy V_0 where $V_0 > E$. This is because, in the classical perspective, we know that the $E_K + E_P = E_T$ where P, K, and T stand for "potential", "kinetic," and "total" respectively, must maintain a measurable total energy which is constant.

With the basics in mind, let us now consider the barrier system. If the particle were to cross from a ground area (where $E_P = 0$) into the forbidden area of the barrier where $E_K < V_0 = E_P$, energy conservation dictates that $E_K < 0$. Both classically and quantum mechanically, this concept of negative energy is undesirable. Classically, this precludes the particle from over crossing the barrier because in order for it to cross it must exist within the barrier and subsequently possess negative kinetic energy. Yet, electronic tunneling is a measurable occurrence.

In Quantum Mechanics there is a principle describing the inherent uncertainty of the universe: the Heisenberg Uncertainty Principle. While it can be formulated in different forms, the one of interest is formulated as follows [1]:

$$\Delta x \Delta p > \frac{\hbar}{2} \tag{1}$$

The basic statement is that momentum and position cannot both be known at the same time with arbitrary precision. In our particular example, we can equate momentum with kinetic energy (if we know one, then we know the other with arbitrary precision), and therefore Heisenberg's uncertainty principle states that we cannot know both the kinetic energy and position.

The particle *can* tunnel without a violation of conservation of energy. Any attempt to precisely measure the kinetic energy of the particle leads to uncertainty in the location of the particle (is it in the barrier or not?). Measuring the location of the particle leads to uncertainty in the kinetic energy, therefore even if we measure the particle to be located in the barrier, the kinetic energy will be unknown. No violation of our intuitive understanding of the world occurs.

3.1 General Mathematical Foundations

In this section, we explore the general mathematical foundations used in this paper for a free particle barrier system. We begin with the general Schroedinger Equation of a system [1]:

$$\begin{aligned} \hat{\boldsymbol{H}}\Psi(x) = \underbrace{-\frac{\hbar^2}{2m}\frac{\partial^2}{\partial x^2}}_{KE}\Psi(x) + \underbrace{V(x)}_{PE}\Psi(x) = \hat{\boldsymbol{E}}\Psi(x) = & \underbrace{E\Psi(x)}_{time-independent} && (2) \\ & = \underbrace{\hat{\boldsymbol{E}}\Psi(x) = i\hbar\frac{\partial}{\partial t}\Psi(x)}_{time-dependent} && (3) \end{aligned}$$

As can be seen, the equation is written in one dimension with the assumption that the total energy of the particle, E, is equal to the sum of the kinetic energy KE (dependent on position x) and the potential energy PE (also dependent on position). Intuitively, this makes sense because the only energies contributing to a particles motion in a transistor are kinetic and potential. Furthermore, we demonstrate one-dimensional solutions because the generalization to greater dimensions will only serve to unnecessarily complicate the mathematics without providing much gained understanding of the electronic tunneling effect.

We begin by noting that the model is essentially separated into three discrete regions: Region 1 is the region where the particle freely exists (in our case, Region 1 is the gate), Region 2 is the increased potential region due to the barrier (in our case, Region 2 models the insulating layer), and Region 3 is the classically inaccessible region (into which we tunnel, and in our case Region 3 models the conductive channel). In the general case, let the wave-function for our particle in Region 1 be $\Psi_1(x)$, in Region 2 $\Psi_2(x)$, and in Region 3 $\Psi_3(x)$. Then the wave-function for a particle in this system is given by the following piece-wise function:

$$\Psi(x) = \begin{cases} \Psi_1(x) & : x < 0 \\ \Psi_2(x) & : 0 \leq x \leq L \\ \Psi_3(x) & : x > L \end{cases} \tag{4}$$

Now, the function must be "well-behaved" in order for it to represent a particle. Mathematically this means that $\Psi(x)$ must be a continuous differentiable function with a continuous first derivative. In other words, we have the following general restrictions:

$$\Psi_1(0) = \Psi_2(0) \tag{5}$$

$$\Psi_2(L) = \Psi_3(L) \tag{6}$$

$$\frac{\partial}{\partial x}\Psi_1(x)\bigg|_{x=0} = \frac{\partial}{\partial x}\Psi_2(x)\bigg|_{x=0} \tag{7}$$

$$\frac{\partial}{\partial x}\Psi_2(x)\bigg|_{x=L} = \frac{\partial}{\partial x}\Psi_3(x)\bigg|_{x=L} \tag{8}$$

Finally, we note that due to the nature of a wave-function, once appropriate solutions for Equation 2 are found, solutions for 3 take the following form:

$$\Psi(x,t) = \Psi(x)\mathrm{e}^{-iwt} \tag{9}$$

Where $w = \frac{E}{\hbar}$ and e is Euler's constant. The above mathematics is sufficient for the analysis of the system discussed in this paper.

3.2 Free Particle Tunneling Barrier Model

First, we analyze the described particle barrier model under the assumptions that the particle is traveling through free space before and after encountering the barrier. We do this because the analysis requires none of advanced mathematics usually associated with finding solutions for an arbitrary Schroedinger Equation, Equation 2.

At first, this model might appear severely restricted because it is clear that electrons don't travel through free space in a MOSFET system, but when considering a single electron, as is done here, the assumption that the interactions with other particles is minimal is valid. A single electron traveling through a conductive material, such as that which resides in both the gate and conductive channel, is basically unfettered in its motion and can be closely approximated by a free-particle model.

3.2.1 Modeling Regions

We begin with a relatively simple analysis of a particle barrier system with homogeneous non-barrier regions. Figure 3 clarifies this description.

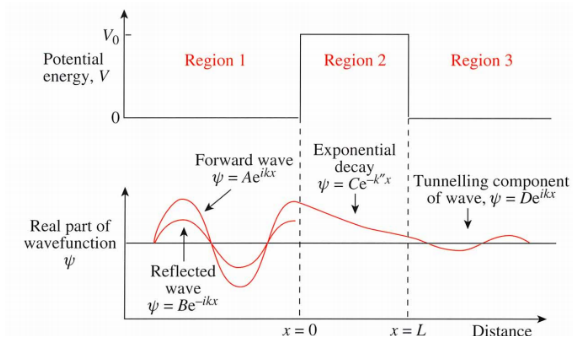

Figure 3: Model for a free particle barrier system. The particle behaves freely along Region 1, with no additional restriction. In Region 2 we have $E - V < 0$, therefore the wavefunction for the particle undergoes exponential decay. In Region 3 we once again model a particle with no restrictions. Note the symmetry in Region 1 and 3. This is a homogeneous square barrier system (ie $V_1 = V_3$.)

Mathematically, the potential in Figure 3 is described as follows:

$$V(x) = \begin{cases} 0 & : x < 0 \text{ or } x > L \\ V_0 & : 0 \leq x \leq L \end{cases} \tag{10}$$

Hayward has a detailed description of this model [1], and here we follow a similar approach to derive the tunneling probability. One significant difference in our approach, though, is the fact that we match not only the wavefunctions but also their derivatives at turning points. Other smaller differences will be described as we proceed.

3.2.2 Mathematics Behind Regions

Looking at Region 1 in Figure 3 and at Equation 2, we have the following:

$$-\frac{\hbar^2}{2m}\frac{\partial^2}{\partial x^2}\Psi_1(x) + V(x)\Psi_1(x) = E\Psi_1(x)$$
$$-\frac{\hbar^2}{2m}\frac{\partial^2}{\partial x^2}\Psi_1(x) - E\Psi_1(x) = 0$$

This is a second-order homogeneous partial differential equation, with a characteristic polynomial with complex roots, and therefore the solution is

$$\Psi_1(x) = Ae^{ik_1x} + Be^{-ik_1x} \tag{11}$$

Where $k_1 = \frac{\sqrt{2mE}}{\hbar}$ and A and B are complex normalization constants. Intuitively, this solution makes sense. The part of the wave with forward momentum is Ae^{ik_1x} while the part reflected back is Be^{-ik_1x}. The i in each exponential implies the wave-nature of the system.

Now for Region 2. Similarly, we have the following:

$$-\frac{\hbar^2}{2m}\frac{\partial^2}{\partial x^2}\Psi_2(x) + V(x)\Psi(x) = E\Psi_2(x)$$
$$-\frac{\hbar^2}{2m}\frac{\partial^2}{\partial x^2}\Psi_2(x) + (V_0 - E)\Psi_2(x) = 0$$

This is a second-order homogeneous partial differential equation. Note that $V_0 > E$, and therefore the characteristic polynomial of this differentiable equation has real roots. We then have:

$$\Psi_2(x) = C\mathrm{e}^{k_2 x} + D\mathrm{e}^{-k_2 x} \tag{12}$$

Where $k_2 = \frac{\sqrt{2m(V_0-E)}}{\hbar}$ and C and D are complex normalization constants. Note that this form of the equation differs significantly from the one shown in Hayward [1].

Lastly, Region 3 in the homogeneous case is remarkably similar to Region 1. One slight difference is that there is no "reflected" wave due to the lack of another barrier.

$$\Psi_3(x) = E\mathrm{e}^{ik_3 x} + F\mathrm{e}^{-ik_3 x} \tag{13}$$

Where $F = 0$, for the reasons explained above, and $k_3 = k_1$ because both Region 1 and Region 3 have the same potentials.

We now proceed to apply the restriction described in Equations 5, 6, 7, and 8. We do this in a slightly more general fashion then required in order to avoid repeating the calculation later.

Applying Equations 5 and 7 yields the following equations:

$$A + B = C + D$$
$$ik_1 A - ik_1 B = k_2 C - k_2 D$$

Solving for A and B (this can be done with matrix inversion using some basic linear algebra techniques)

$$A = \frac{(k_2 + ik_1)}{2ik_1}C - \frac{(k_2 - ik_1)}{2ik_1}D \tag{14}$$
$$B = -\frac{(k_2 - ik_1)}{2ik_1}C + \frac{(k_2 + ik_1)}{2ik_1}D \tag{15}$$

Similarly, applying 6 and 8 yield the following equations:

$$C\mathrm{e}^{k_2 L} + D\mathrm{e}^{-k_2 L} = E\mathrm{e}^{ik_3 L} + F\mathrm{e}^{-ik_3 L}$$
$$k_2 C\mathrm{e}^{k_2 L} - k_2 D\mathrm{e}^{-k_2 L} = ik_3 E\mathrm{e}^{ik_3 L} - ik_3 F\mathrm{e}^{-ik_3 L}$$

Again, with some basic linear algebra techniques it's relatively effortless to solve the above for C and D.

$$C = \frac{(k_2 + ik_3)\mathrm{e}^{(ik_3 - k_2)L}}{2k_2}E + \frac{(k_2 - ik_3)\mathrm{e}^{-(ik_3 + k_2)L}}{2k_2}F \tag{16}$$
$$D = \frac{(k_2 - ik_3)\mathrm{e}^{(ik_3 + k_2)L}}{2k_2}E + \frac{(k_2 + ik_3)\mathrm{e}^{-(ik_3 - k_2)L}}{2k_2}F \tag{17}$$

We now have A and B in terms of C and D which are in terms of E and F. Recalling that A and B relate to Region 1, and E and F to Region 3, by combining the Equation 14 with 16 and 17 and similarly for Equation 15 we can arrive at a two equations relating Region 1 to Region 3. We have:

$$A = (M_{A,C}M_{C,E} + M_{A,D}M_{D,E})E + (M_{A,C}M_{C,F} + M_{A,D}M_{D,F})F$$
$$B = (M_{B,C}M_{C,E} + M_{B,D}M_{D,E})E + (M_{B,C}M_{C,F} + M_{B,D}M_{D,F})F$$

Where $M_{\alpha,\beta}$ is the coefficient on β from the equation with α on the left hand side.

For conciseness, we now set the following relations:

$$\begin{aligned} M_{A1} &= M_{A,C}M_{C,E} + M_{A,D}M_{D,E} \\ M_{A2} &= M_{A,C}M_{C,F} + M_{A,D}M_{D,F} \\ M_{B1} &= M_{B,C}M_{C,E} + M_{B,D}M_{D,E} \\ M_{B2} &= M_{B,C}M_{C,F} + M_{B,D}M_{D,F} \end{aligned}$$

Therefore, we can now write A and B in terms of E and F succinctly:

$$A = M_{A1}E + M_{A2}F \tag{18}$$
$$B = M_{B1}E + M_{B2}F \tag{19}$$

3.2.3 Application to Homogeneous Regions

Having solved in the general sense, we know return to our particular problem. Note that, as discussed above, $F = 0$.

We are interested in calculating the probability of a particle ending up in Region 3. By a similar argument to those made by Simmons [2], Hayward [1], Lee [11], and Salas [9], we can determine the tunneling probability by considering the fact that the electrons going into the barrier are proportional to $|\Psi_1(x)|^2$ (where $\Psi_1(x)$ is the incidence wave) and the electrons leaving the barrier proportional to $|\Psi_3(x)|^2$. Therefore, the probability of an electron tunneling is

$$\begin{aligned} P &= \frac{|\Psi_3(x)|^2}{|\Psi_1(x)|^2} \\ &\approx \frac{E^*E\mathrm{e}^{ik_3x}\mathrm{e}^{-ik_3x}}{A^*A\mathrm{e}^{ik_1x}\mathrm{e}^{-ik_1x} + B^*B\mathrm{e}^{ik_1x}\mathrm{e}^{-ik_1x}} && \text{(assuming A and B are normalized)} \\ &= \frac{|E|^2}{|A|^2 + |B|^2} \end{aligned}$$

Using Equation 18 and 19 (with $F = 0$) we have

$$P = \frac{1}{|M_{A1}|^2 + |M_{B1}|^2} \tag{20}$$

We now focus our attention on calculating M_{A1} and M_{B1} in terms of the barrier and particle properties. We do this more generally than strictly necessary in order to avoid repeating the calculation later. We have:

$$
\begin{aligned}
M_{A1} &= M_{A,C}M_{C,E} + M_{A,D}M_{D,E} \\
&= \frac{(k_2+ik_1)(k_2+ik_3)}{4ik_1k_2}\mathrm{e}^{(ik_3-k_2)L} - \frac{(k_2-ik_1)(k_2-ik_3)}{4ik_1k_2}\mathrm{e}^{(ik_3+k_2)L} \\
&= \left[\frac{k_2^2-k_1k_3+i(k_1k_2+k_2k_3)}{4ik_1k_2}\mathrm{e}^{-k_2L} - \frac{k_2^2-k_1k_3-i(k_1k_2+k_2k_3)}{4ik_1k_2}\mathrm{e}^{k_2L}\right]\mathrm{e}^{ik_3L} \\
&= \left[i\left(\frac{k_2^2-k_1k_3}{2k_1k_2}\right)\left(\frac{\mathrm{e}^{k_2L}-\mathrm{e}^{-k_2L}}{2}\right) + \frac{(k_1+k_3)\mathrm{e}^{k_2L}+(k_1+k_3)\mathrm{e}^{-k_2L}}{4k_1}\right]\mathrm{e}^{ik_3L}
\end{aligned}
$$

Note that we can use hyperbolic function to simplify a bit further, even in the general case.

$$
= \left[i\left(\frac{k_2^2-k_1k_3}{2k_1k_2}\right)\sinh(k_2L) + \frac{(k_1+k_3)}{2k_1}\cosh(k_2L)\right]\mathrm{e}^{ik_3L} \tag{21}
$$

Similarly, for M_{B1}, noting that $M_{A,C} = M_{B,D}$ and $M_{A,D} = M_{B,C}$

$$
\begin{aligned}
M_{B1} &= M_{B,C}M_{C,E} + M_{B,D}M_{D,E} \\
&= M_{A,D}M_{C,E} + M_{A,C}M_{D,E} \\
&= -\frac{(k_2-ik_1)(k_2+ik_3)}{4ik_1k_2}\mathrm{e}^{(ik_3-k_2)L} + \frac{(k_2+ik_1)(k_2-ik_3)}{4ik_1k_2}\mathrm{e}^{(ik_3+k_2)L} \\
&= \left[-\frac{k_2^2+k_1k_3+i(-k_1k_2+k_2k_3)}{4ik_1k_2}\mathrm{e}^{-k_2L} + \frac{k_2^2+k_1k_3-i(-k_1k_2+k_2k_3)}{4ik_1k_2}\mathrm{e}^{k_2L}\right]\mathrm{e}^{ik_3L} \\
&= \left[-i\left(\frac{k_2^2+k_1k_3}{2k_1k_2}\right)\left(\frac{\mathrm{e}^{k_2L}-\mathrm{e}^{-k_2L}}{2}\right) + \frac{(k_1-k_3)\mathrm{e}^{k_2L}+(k_1-k_3)\mathrm{e}^{-k_2L}}{4k_1}\right]\mathrm{e}^{ik_3L}
\end{aligned}
$$

We can simplify this using hyperbolic functions.

$$
= \left[\frac{(k_1-k_3)}{2k_1}\cosh(k_2L) - i\left(\frac{k_2^2+k_1k_3}{2k_1k_2}\right)\sinh(k_2L)\right]\mathrm{e}^{ik_3L} \tag{22}
$$

We now proceed to calculate $|M_{A1}|^2$ and $|M_{B1}|^2$.

$$
\begin{aligned}
|M_{A1}|^2 &= M_{A1}^*M_{A1} \\
&= \left[-i\left(\frac{k_2^2-k_1k_3}{2k_1k_2}\right)\sinh(k_2L) + \frac{(k_1+k_3)}{2k_1}\cosh(k_2L)\right]\cdot\left[i\left(\frac{k_2^2-k_1k_3}{2k_1k_2}\right)\sinh(k_2L) + \frac{(k_1+k_3)}{2k_1}\cosh(k_2L)\right] \\
&= \left(\frac{k_1+k_3}{2k_1}\right)^2\cosh^2(k_2L) + \left(\frac{k_2^2-k_1k_3}{2k_1k_2}\right)^2\sinh^2(k_2L) \\
&= \left(\frac{k_1+k_3}{2k_1}\right)^2 + \left(\frac{k_1+k_3}{2k_1}\right)^2\sinh^2(k_2L) + \left(\frac{k_2^2-k_1k_3}{2k_1k_2}\right)^2\sinh^2(k_2L) \\
&= \left(\frac{k_1+k_3}{2k_1}\right)^2 + \left[\left(\frac{k_1+k_3}{2k_1}\right)^2 + \left(\frac{k_2^2-k_1k_3}{2k_1k_2}\right)^2\right]\sinh^2(k_2L)
\end{aligned}
$$

A similar process yields $|M_{B1}|$. This gives us the general formulas:

$$|M_{A1}|^2 = \left(\frac{k_1+k_3}{2k_1}\right)^2 + \left[\left(\frac{k_1+k_3}{2k_1}\right)^2 + \left(\frac{k_2^2-k_1k_3}{2k_1k_2}\right)^2\right]\sinh^2(k_2L) \tag{23}$$

$$|M_{B1}|^2 = \left(\frac{k_1-k_3}{2k_1}\right)^2 + \left[\left(\frac{k_1-k_3}{2k_1}\right)^2 + \left(\frac{k_2^2+k_1k_3}{2k_1k_2}\right)^2\right]\sinh^2(k_2L) \tag{24}$$

With some more algebraic manipulation, and recalling that for the homogeneous case we have $k_1 = k_3$, this simplifies down to the following:

$$|M_{A1}|^2 = 1 + \left(\frac{k_2^2+k_1^2}{2k_1k_2}\right)^2 \sinh^2(k_2L) \tag{25}$$

$$|M_{B1}|^2 = \left(\frac{k_2^2+k_1^2}{2k_1k_2}\right)^2 \sinh^2(k_2L) \tag{26}$$

Plugging Equation 25 into Equation 20, we *finally* arrive at the tunneling probability in terms of physical parameters.

$$P = \frac{1}{1+\left(\frac{k_2^2+k_1^2}{2k_1k_2}\right)^2\sinh^2(k_2L)} \tag{27}$$

Where, recall, $k_1 = \frac{\sqrt{2mE}}{\hbar}$ and $k_2 = \frac{\sqrt{2m(V_0-E)}}{\hbar}$. Plugging these values we arrive at the simplest form possible for the probability of tunneling in a free-particle/barrier system with homogeneous regions:

$$P = \frac{1}{1+\frac{V_0^2}{4E(V_0-E)}\sinh^2(k_2L)} \tag{28}$$

3.2.4 Application to Inhomogeneous Regions

As mentioned in Section 3.2.2, the mathematical process described was more general than strictly necessary for a simple model with a symmetric potential landscape. In this section, we focus on inhomogeneous regions (ie, non-symmetric) as seen in Figure 4. The general mathematics used remains the same.

We begin by noting that without loss of generality we can set one of the regions to zero potential (essentially, we are picking our "ground"). The choice is arbitrary, but for the rest of the discussion we will use Region 1 as our ground, therefore $V_1 = 0$. This gives rise to the following wave numbers, corresponding to $\Psi_1(x), \Psi_2(x)$, and $\Psi_3(x)$ respectively:

$$k_1 = \frac{\sqrt{2mE}}{\hbar} \tag{29}$$

$$k_2 = \frac{\sqrt{2m(V_2-E)}}{\hbar} \tag{30}$$

$$k_3 = \frac{\sqrt{2m(E-V_3)}}{\hbar} \tag{31}$$

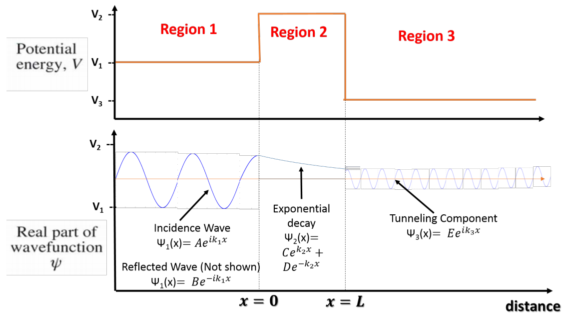

Figure 4: Free particle/barrier inhomogeneous region system. The model consists of three regions, each at different potentials. The middle region is always at the highest potential, and is therefore the "barrier". Region 1 is always the originator region, while Region 3 the receiving region. As can be seen, each region has its own potential and is therefore a generalization Section 3.2.3

Plugging Equations 29, 30, and 31 into Equation 23 and 24 we have:

$$|M_{A1}|^2 = \left(\frac{E+\sqrt{E(E-V_3)}}{2E}\right)^2 + \left[\left(\frac{E+\sqrt{E(E-V_3)}}{2E}\right)^2 + \frac{((V_2-E)-\sqrt{E(E-V_3)})^2}{4E(V_2-E)}\right]\sinh(k_2L)$$

$$|M_{B1}|^2 = \left(\frac{E-\sqrt{E(E-V_3)}}{2E}\right)^2 + \left[\left(\frac{E-\sqrt{E(E-V_3)}}{2E}\right)^2 + \frac{((V_2-E)+\sqrt{E(E-V_3)})^2}{4E(V_2-E)}\right]\sinh(k_2L)$$

With some messy algebra and simplification and plugging in our result into Equation 20, we arrive at the following equation. Note that, as a sanity check, we can plug in $V_2 = V_0$ and $V_3 = 0$ and verify that we do in fact obtain Equation 28. Fantastic!

$$P = \frac{1}{1 - \frac{V_3}{2E} + \left(\frac{(V_2-V_3)V_2}{4E(V_2-E)}\right)\sinh(k_2L)} \tag{32}$$

3.3 Computational Analysis of Parameter Effects

We now turn our attention to determining the effect of changes in different parameters on the tunneling probability. In order to analyze the probability, we use Matlab to compute changes in probability due to variations in input parameters. The main sections of code can be found in Section 5 on Page 17.

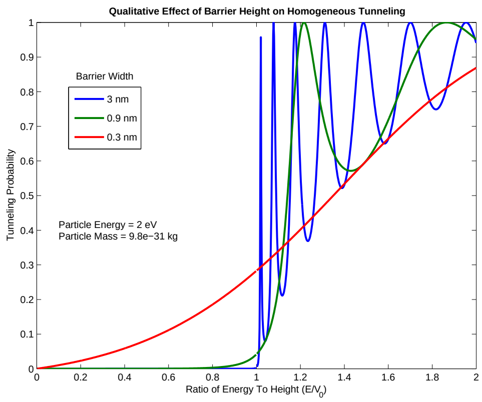

Figure 5: Tunneling Probability vs Particle Energy to Barrier Height Ratio. When the $E < V_0$, the tunneling depends heavily of the width of the potential barrier. For relatively small widths when (red), we can see that there is a significant level of tunneling. As the width of the barrier increases (green and blue) the tunneling decreases exponentially. For $E > V_0$ the tunneling, as expected, is significant.

3.3.1 Homogeneous Region Computations

From the Equation 28 we can expect the following:

- The barrier:

  1. As the width of the barrier, L, increases, $\sinh^2(k_2 L)$ increases exponentially and therefore P decreases exponentially. The converse also appears to be true. This can bee seen in Figure 5, and more directly in Figure 8 on page 15. Of interest is the sudden spike that occurs for the wide barriers as soon as $E > V_0$. Note that for the thinnest barrier, the probability when $E > V_0$ tends to remain below that of the others. This can be explained by the fact that the wavefunction can resonate with the barrier. If the wavelength matches the width of the barrier just right (ie, $\frac{n\lambda}{2} = w$ for some $n \in \mathbb{Z}$), then the wavefunction will be almost completely unaffected by the existence of the barrier. Otherwise, the particle still "feels" the presence of the barrier as a decay in its amplitude. This can also be gathered from Figure 8 by nothing the periodicity of all $V_0 < E$.
  2. As the square of the potential height of the barrier, V_0^2 increases, k_2 increases almost proportionally. This should lead to an exponential increase in $\sinh^2(k_2 L)$, leading to an exponential decay of P. The converse also appears to be true. This can be seen in Figure 5, but for a better look see Figure 6 on Page 22.

- The particle:

  1. As the kinetic energy of the particle, E, increases, k_1 increases and k_2 decreases. This should lead to an increase in P. Yet, not that when $E = V_0$, Equation 28 is undefined. Nonetheless, the function is *not* discontinuous. As can be seen in Figure 5, our prediction matches the collected data.
  2. As the mass of the particle, m, increases, k_1 and k_2 both increase. This should lead to a decay in tunneling probability. This result is shown for $E < V_0$ in Figure 6. At the end of the paper, Figure 6 shows the results when $E > V_0$, but this isn't of particular interest for the current discussion. Note that Figure 6 holds the particle energy. Effectively, this is a function of wavelength then. For comparison, note Figure 6 where the energy is once again held constant. Why do the two figures look so different? Note the change in scales,

and the fact that $m \propto \frac{1}{\lambda}$, so the behavior of the two plots is reversed. Taken together, the plots support the statement that as m increases (or λ decreases), the probability of tunneling decreases. This might seem counterintuitive, but recall that we are holding the energy of the particle constant (almost an artificiality).

For the case where we do not hold the energy of the particle constant, a view at Figure 7 shows the reverse effect. Increasing the wavelength decreases the energy of the particle, therefore the tunneling probability declines. Note that a plot where the mass is changed and the wavelength is held constant would simply be the reverse of the one in the Figure.

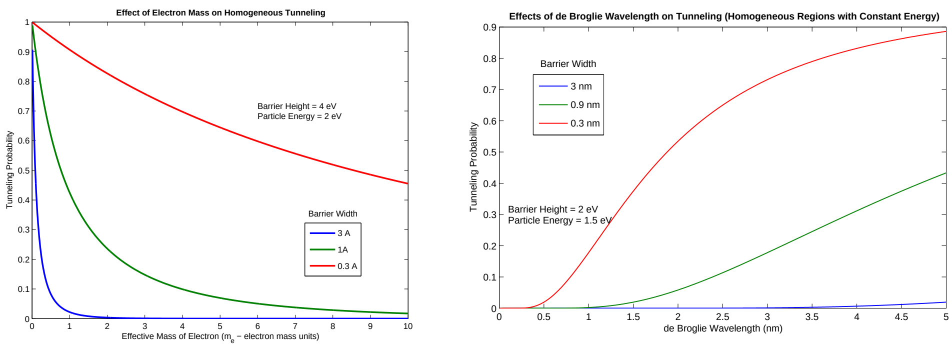

Figure 6: Probability vs Particle Mass/Wavelength for Fixed Energy. The data shown on the right plot is artificial in the sense that it is difficult to think of a scenario where changing the wavelength does not in some way affect that mass and evergy of a particle wouldn't affect the energy, but nonetheless the figures serve to verify the prediction by Equation 28.

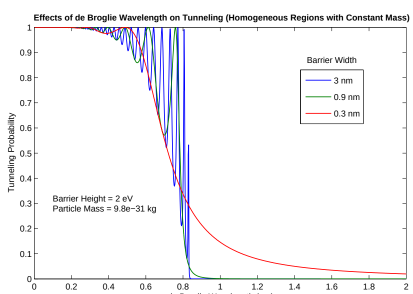

Figure 7: Probability vs Particle Wavelength with Varying Energy. Of note is that this is, essentially, the same as the plotting against energy. This makes sense because an increase in wavelength leads to a decrease in energy.

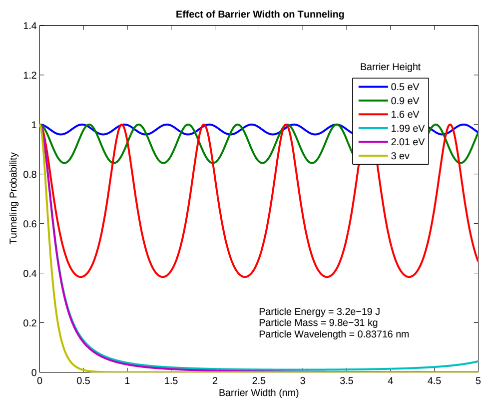

Figure 8: Probability vs Barrier Width for Constant Energy and Mass. Note that blue, green, and red are all systems where $E > V_0$. Interesting to note is that the particle still feels the effects of the barrier, but when the wavelength matches the width of the barrier, then the particle feels almost no effect from the barrier. For the others, the behavior is as expected.

3.3.2 Inhomogeneous Region Computations

Considering that the above is a special case of this model, then we can expect similar results. In addition, from Equation 32 we can expect the following:

- If $V_3 > V_1$, then in our model $V_3 > 0$ and it has an nullifying effect on the coefficient for sinh. Therefore, the tunneling probability should increase linearly with increasing V_3.
- If $V_3 < V_1$, then in our model $V_3 < 0$ and it has an amplifying effect on the coefficient for sinh. Therefore, the tunneling probability should decrease linearly with decreasing V_3.

Both of the above predictions, are not surprisingly, matched. The probability functions for kinetic energy (Figure 3.3.2), wavelength with variable energy (Figure 3.3.2) and wavelength with constant energy (Figure 3.3.2). Given more time, these should be explored further.

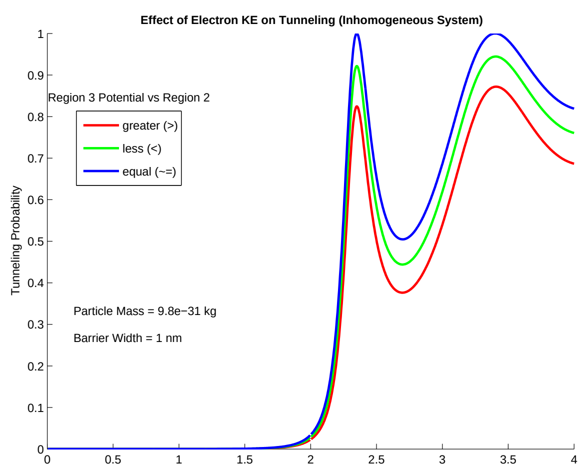

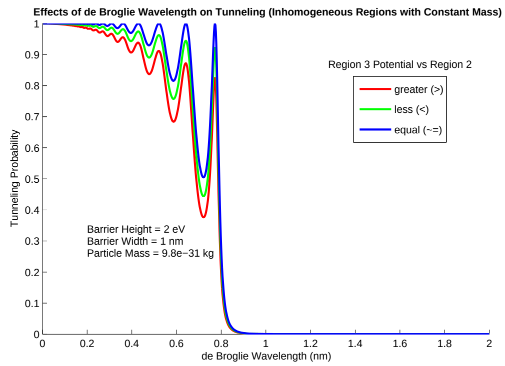

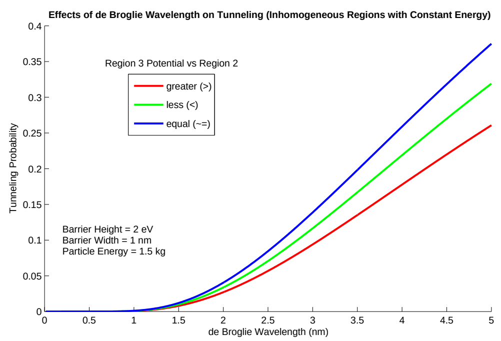

4 Conclusion

Tunneling probability depends heavily both on barrier width and barrier height. These two model parameters are directly correlated with the thickness of an insulating film in a transistor, as well as with the dielectric constant of the insulating material [2]. Varying these too parameters towards thicker insulating materials with higher dielectric constants will lead, as shown, to quantitatively fewer electron tunneling to the unwanted reagion (Region 3, in our case). This agrees with what has been shown in the literature [7] [8].

In the paper we specify not only a general formula for the tunneling probability (Equation 28) with homogeneous regions (where V_0 is the the barrier height) but we also do a more general analysis for the case of inhomogeneous regions. This analysis yield Equation 32.

The analysis focuses on providing an intuitive understanding for the homogeneous regions model, and in providing comparison to the inhomogeneous region model. In particular, the focus is in the cases where the voltage of Region 3 is below that of Region 1 (ie, $V_3 < V_1$). This is becase for a transistor, the channel is usually at a lower voltage than the gate (it is an increase in voltage that causes the transistor to turn on).

Despite the above, it seems that changes in V_3 do not affect the tunneling probability of electrons significantly. Instead, the effect seems to be linear and symmetric about the barrier height. It is also possible that the derivations presented lead to an incorrect formula due to the assumptions made about the shape of the wavefunction in each region. This is unlikely, but due to the counterintuitive nature of the results, an area of research which should be explored further.

5 Matlab Code

Here we provide a quick glance at some of the source code used for the calculations presented in the paper, in addition to the generation of figures and graphs. It should be noted that the code is only an implementation of the mathematics explained in section 3.2.2 on page 7.

This is `main.m`, the Matlab file which executes the bulk of the calculations. It is written sequentially and without regard for extendability.

```matlab
% Setup environment
close all;
clear all;

% Add ability to export to powerpoint
if exist('pptfigure','file')
    pptfigure on;
end;

% Recall that physical constants are all defined in Physics.m
mass = Physics.emass;
c = Physics.c;
hbar = Physics.hbar;
% Widths of barrier and mass of electron
widthsE = [3e-9 9e-10 3e-10]; % 3nm, 0.9nm, and 0.3nm
me = mass;

% Kinetic energy for electron varies from tiny eV to 4 eV
lastE = 4 * Physics.eV;
deltaE = lastE / Constants.datapoints;
E = deltaE:deltaE:lastE;

% Potential barrier height is 1/2 the maximum KE
V0 = max(E)/2;

% Calculate the wavenumbers and tunneling probability
k1 = sqrt(2 * me * E) / hbar;
k2 = sqrt(2 * me * (V0 - E)) / hbar;
probE = tunnelingP(widthsE,k1,k2);

% Plot the three graphs on one figure for P vs E (eV)
figure(1);
plot(E / Physics.eV, probE,'LineWidth',Constants.lwidth);

% Creating V3
V0 = 2 * Physics.eV;
V3 = [-V0/2 -V0/5 0];
colors = {'red','green','blue'};

% Barrier width
L = 1e-9 ; % m

% Calculate and plot
figure(2);
hold on;
for n = 1:length(V3)
    k3 = sqrt(2 * me * abs(E - V3(n))) / hbar;
    probIE = tunnelingP(L,k1,k2,k3);
```

```
    plot(E / Physics.eV,probIE(:,1),colors{n},'LineWidth',Constants.lwidth);
end;
%%%%%%%%%%%%%%%%%%%%%%%%%%%%%%%%%%%%%%%%%%%%%%%%%%%%%%%%%%%%%%%%%%%%%%%%%%%

% calculate wavelengths
lastL = 2 * 1e-9; % 5nm
deltaK =  lastL / Constants.datapoints; % max is 5nm
lambda = (deltaK:deltaK:lastL); % m

% Calculate energies
EL = (Physics.h ./ lambda) .^ 2 ./ (2 * me);
k1 = 2*pi * (1./ lambda);
k2 = sqrt(2 * me * (V0 - EL)) / hbar;

% recalculate prob
probE2 = tunnelingP(widthsE,k1,k2);

% Plot the three graphs as a function of wavelenths (P vs \lamda)
figure(3);
plot(lambda * 1e9,probE2,'LineWidth',Constants.lwidth - 1);
% Calculate and plot
figure(4);
hold on;
for n = 1:length(V3)
    k3 = sqrt(2 * me * (EL - V3(n))) / hbar;
    probIL = tunnelingP(L,k1,k2,k3);
    plot(lambda * 1e9,probIL(:,1),colors{n},'LineWidth',Constants.lwidth);
end;
hold off;

% calculate wavelengths
lastL = 5 * 1e-9; % 5nm
deltaK =  lastL / Constants.datapoints; % max is 5nm
lambda2 = (deltaK:deltaK:lastL); % m

% Calculate masses
E0L = 1.5 * Physics.eV;
ML = Physics.h ^ 2 ./ (2 * lambda2 .^2 * E0L);
k1 = 2*pi * (1./ lambda2);
k2 = sqrt(2 * ML * (V0 - E0L)) / hbar;

% recalculate prob
probE3 = tunnelingP(widthsE,k1,k2);

% Plot the three graphs as a function of wavelenths (P vs \lambda)
figure(5);
plot(lambda2 * 1e9,probE3,'LineWidth',Constants.lwidth - 1);
% Calculate and plot
figure(6);
hold on;
for n = 1:length(V3)
    k3 = sqrt(2 * ML * (E0L - V3(n))) / hbar;
    probIL2 = tunnelingP(L,k1,k2,k3);
    plot(lambda2 * 1e9,probIL2(:,1),colors{n},'LineWidth',Constants.lwidth);
end;
hold off;
% Barrier height varies from tiny eV to 4 eV
lastV = 4 * Physics.eV;
```

```
deltaV = lastV / Constants.datapoints;
V = deltaV:deltaV:lastV;

% Set kinetic energy at half the barrier height
E0 = max(V)/2;

% Calculate the tunelling probability
k1 = sqrt(2 * me * E0) / hbar * ones(1,length(V));
k2 = sqrt(2 * me * (V - E0)) / hbar;
probV = tunnelingP(widthsE,k1,k2);

% Plot the three graphs on one figure for P vs E
figure(7);
plot(V / Physics.eV, probV,'LineWidth',Constants.lwidth);
% Plot as E/V0 ratio (ie, energy to barrier height)
figure(8);
V0 = max(E) /2;
plot((E ./ V0), probE,'LineWidth',Constants.lwidth);

% Set the three heights and the particle energy
heightsW = [0.5 .9 1.6 1.99 2.01 3] * Physics.eV;
E0 = 2.0 * Physics.eV; % right on middle barrier

% Use widths varying from tiny to 20nm
lastW = 5e-9; % 5 nm
deltaW = lastW / Constants.datapoints;
widthsW = 0:deltaW:lastW;

% Calculate homogeneous system constants
k1 = sqrt(2 * mass * E0) / hbar * ones(1,length(heightsW));
k2 = sqrt(2 * mass * (heightsW - E0)) / hbar;
probW = tunnelingP(widthsW,k1,k2)'; % So prob (:,1) gives the prob for k1(1) and k2(1)

% Plot all graphs
figure(9);
plot(widthsW * 1e9,probW,'LineWidth',Constants.lwidth);

% mass of electron varies from 0.01 effectiveness to 10
lastM = 10 * mass;
deltaM = lastM / Constants.datapoints;
M = deltaM:deltaM:lastM;

% Potential barrier height is twice the KE, which is 2 eV
E0 = 2 * Physics.eV;
V0 = 2*E0;

% Calculate the tunelling probability
k1 = sqrt(2 * M * E0) / hbar;
k2 = sqrt(2 * M * (V0 - E0)) / hbar;
probM = tunnelingP(widthsM,k1,k2);

% Plot the three graphs on one figure for P vs M
figure(10);
plot(M / mass, probM,'LineWidth',Constants.lwidth);
E0 = 2 * Physics.eV;
V0 = E0 / 2;

% Calculate the tunelling probability
```

```
k1 = sqrt(2 * M * E0) / hbar;
k2 = sqrt(2 * M * (V0 - E0)) / hbar;
probM2 = tunnelingP(widthsE,k1,k2);

% Plot the three graphs on one figure for P vs M
figure(11);
plot(M / mass, probM2,'LineWidth',Constants.lwidth);
```

Next, we have `Constants.m`. This file includes all arbitrarily defined constants used in the calculations.

```
classdef Constants
    properties ( Constant = true)
        deltat = 1/100; % seconds
        timecycles = 10; % number of cycles for the time dependent wavefunction
        xaxis = -100:0.01:100; % [xmin,xmax,ymin,ymax]
        deltax = 0.01;
        datapoints = 1000; % number of datapoints used in calculations and graphs
        lwidth = 2; % line width parameter for plots
    end
end
```

`Physics.m` provides a nice container for physical constants used in other files.

```
classdef Physics
    properties ( Constant = true)
        h = 6.63e-34; % Js
        hbar = 6.63e-34 / (2*pi);
        c = 3e8; % m/s
        emass = 9.8e-31; %kg
        eV = 1.6e-19 % electron volt
    end
end
```

`tunneling.m` implements the bulk of the complex mathematics explained in Section 3.2.2 on page 7. It is a function for calculating tunneling probabilities.

```
function prob = tunnelingP(L,k1,k2,k3)
% TUNNELINGP: computes the tunneling probability of a particle a across a
% barrier (Region 2) and into Region 3 when originally on Region 1.
    assert(length(k1) == length(k2),'Wavenumbers for Region 1 and 2 do not correspond!');

    % Assume potential landscape is symmetric
    if (nargin == 3)
        k3 = k1;
    end;


    num = length(L);
    xnum = length(k1);
    prob = ones(xnum,num);
    for n = 1:num;
        M_ac = (k2 + 1i * k1) ./ (2 * 1i * k1);
        M_ce = (k2 + 1i * k3) .* exp((1i * k3 - k2) * L(n)) ./ (2 * k2);
```

```
        M_ad = -1 * (k2 - 1i * k1) ./ (2 * 1i * k1);
        M_de = (k2 - 1i * k3) .* exp((1i * k3 + k2) * L(n)) ./ (2 * k2);
        M_a1 = M_ac .* M_ce + M_ad .* M_de;

        M_bc = M_ad;
        M_bd = M_ac;
        M_b1 = M_bc .* M_ce + M_bd .* M_de;

        % Calculate probability
        prob(:,n) = real(1 ./ ((conj(M_a1) .* M_a1) + (conj(M_b1) .* M_b1)));
    end;

end
```

6 Additional Figures

Here are additional figures calculated and superficially referenced in the text.

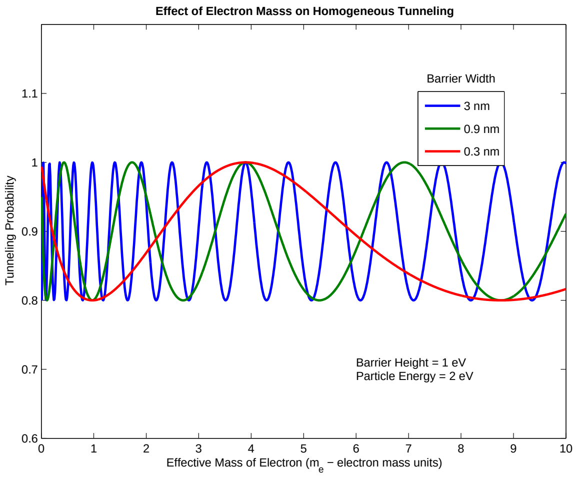

Effect of Electron Masss on Homogeneous Tunneling
Barrier Width
3 nm
0.9 nm
0.3 nm
Barrier Height = 1 eV
Particle Energy = 2 eV
Tunneling Probability
Effective Mass of Electron (m_e − electron mass units)

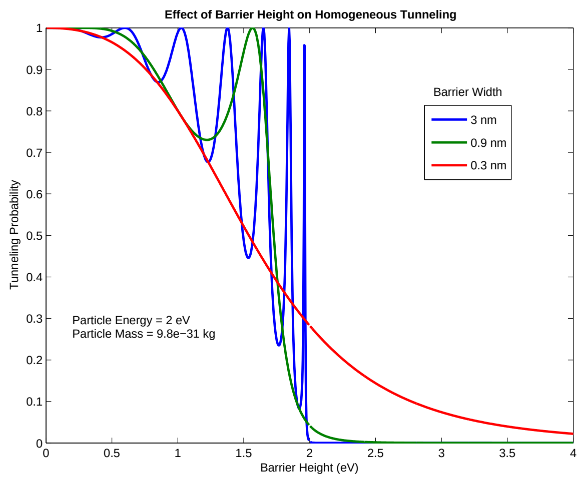

Effect of Barrier Height on Homogeneous Tunneling
Barrier Width
3 nm
0.9 nm
0.3 nm
Particle Energy = 2 eV
Particle Mass = 9.8e−31 kg
Tunneling Probability
Barrier Height (eV)

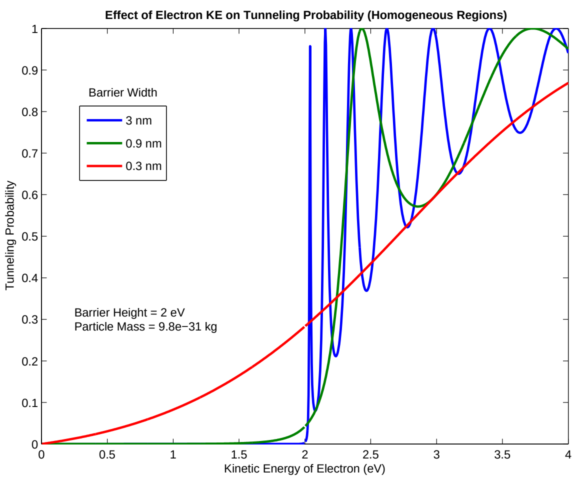

Effect of Electron KE on Tunneling Probability (Homogeneous Regions)
Barrier Width
3 nm
0.9 nm
0.3 nm
Barrier Height = 2 eV
Particle Mass = 9.8e−31 kg
Tunneling Probability
Kinetic Energy of Electron (eV)

References

[1] David O. Hayward. *Quantum Mechanics for Chemists.* The Royal Society of Chemistry, first edition, 2012. pages 58–65, 30–55.

[2] John G. Simmons. Generalized formula for the electric tunnel effect between similar electrodes separated by a thin insulating film. *Applied Physics*, 34(6), January 1963. Web. 1 Nov 2013.

[3] J. Appenzeller, Y.-M. Lin, J. Knoch, and Ph. Avouris. Band-to-band tunneling in carbon nanotube field-effect transistor. *Physical Review Letters*, 93(19), November 2004. Web. 1 Nov 2013.

[4] Adrian M. Ionescu and Heike Riel. Tunnel field-effect transistors as energy-efficient electronic switches. *Nature*, 479(329), November 2011. Web. 4 Nov 2013.

[5] Woo Young Choi, Byung-Gook Park, Jong Duck Lee, and Tsu-Jae King Liu. Tunneling field-effect transistors (TFETs) with subthreshold swing (SS) less than 60 mV/dec. *IEEE Electronic Device*, 28(8), August 2007. Web. 4 Nov 2013.

[6] Community. Quantum tunneling. `http://en.wikipedia.org/wiki/Quantum_tunneling`, November 2013.

[7] Community. Rectangular potential barrier. `http://en.wikipedia.org/wiki/Rectangular_potential_barrier`, November 2013.

[8] Hyper-physics. Barrier penetration. `http://hyperphysics.phy-astr.gsu.edu/hbase/quantum/barr.html`, September 2008.

[9] Christian Salas. Mathematical notes on the schrdinger equation and quantum tunneling. `http://www.drchristiansalas.org.uk/MathsandPhysics/Physics/QuantumTunneling.pdf`, April 2008.

[10] Gordon E. Moore. Cramming more components onto integrated circuits. *Electronics*, 38(8), April 1965. Web. 17 Nov 2013.

[11] Kyu-Tae Lee, Eun Joo Jung, Chul Han Kim, and Chang-Min Kim. Derivation of tunneling probabilities for arbitrarily graded potential barriers using modied airy functions. *Optical and Quantum Electronics*, 42, January 2011. Web. 6 Dec 2013.